Available online at www.sciencedirect.com
ScienceDirect
Radiation Measurements 42 (2007) 1587–1599
Radiation Measurements
www.elsevier.com/locate/radmeas

# Simulations of the effect of pulse annealing on optically-stimulated luminescence of quartz

V. Pagonis[a,*], A.G. Wintle[b], R. Chen[c]

[a]*Physics Department, McDaniel College, Westminster, MD21157, USA*
[b]*Institute of Geography and Earth Sciences, University of Wales, Aberystwyth SY23 3DB, UK*
[c]*School of Physics and Astronomy, Raymond and Beverly Sackler Faculty of Exact Sciences, Tel-Aviv University, Tel-Aviv 69978, Israel*

Received 14 April 2007; accepted 4 September 2007

**Abstract**

Pulse annealing techniques are commonly used in OSL studies of quartz to obtain information on the kinetic parameters of OSL traps and hole reservoirs. In this paper, simulations of pulse annealing experiments are carried out using the comprehensive model for quartz developed by Bailey [2001. Towards a general kinetic model for optically and thermally stimulated luminescence of quartz. Radiat. Meas. 33, 17–45] for both natural and laboratory irradiated aliquots. The results of the simulations are in qualitative agreement with, and reproduce, several unusual features of the experimental data of Wintle and Murray [1998. Towards the development of a preheat procedure for OSL dating of quartz. Radiat. Meas. 29, 81–94]. The simulations are also carried out using different heating rates, and show that pulse annealing experiments can be used to recover appropriate kinetic parameters for both the OSL traps and the hole reservoirs known to exist in quartz. The results of the simulations show the importance of these hole reservoirs in determining how the OSL signal depends upon the preheat temperature.


*Keywords:* OSL; Sensitivity changes; Quartz; Pulse annealing; Lifetime; Activation energy

## 1. Introduction

A pre-measurement thermal treatment during optically-stimulated luminescence (OSL) experiments is useful for isolating thermally stable signals; application of a short thermal treatment (such as 10 s at 260 °C) is commonly employed during dating studies of quartz (e.g. Murray and Wintle, 2000). As a quantitative analytical tool, shorter times and a range of temperatures, have been used to obtain information on the kinetic parameters of OSL traps and hole reservoirs of quartz (Li and Chen, 2001); such a procedure is referred to as pulse annealing (Bailiff and Poolton, 1991). As a diagnostic tool, pulse annealing is valuable in determining the correct thermal treatments to be applied in dating protocols (Bulur et al., 2000). In particular, it can help identify the extent of sensitivity changes taking place during preheating of the samples, to track possible thermal transfer phenomena (Li et al., 2006) and to choose the optimal preheat temperatures for dating protocols.

OSL signals are usually measured after aliquots of quartz have been given a preheat treatment in the laboratory in order to isolate a particular OSL component, e.g. by holding the aliquot for 5 min at temperatures up to 240 °C (Rhodes, 1988). During application of the single-aliquot regenerative-dose (SAR) protocol (Murray and Wintle, 2000), it is necessary to correct the measured OSL signal for the sensitivity changes which take place during preheating of the sample. Several experimental studies have established that these sensitivity changes depend on the radiation history of the sample, on whether the irradiation was carried out in nature or in the laboratory, and on whether the OSL signal was zeroed by optical bleaching before the sample was irradiated in the laboratory (Wintle and Murray, 2006). It is thus important to monitor and correct for sensitivity changes during OSL measurements made during dating applications. This may be carried out using the thermoluminescence (TL) response of the 110 °C TL peak of quartz to a small beta test dose (Murray and Roberts, 1998; Stoneham and Stokes,

* Corresponding author.
*E-mail address:* vpagonis@mcdaniel.edu (V. Pagonis).

1350-4487/$ - see front matter © 2007 Elsevier Ltd. All rights reserved.
doi:10.1016/j.radmeas.2007.09.003

1991; Chen et al., 2000; Chen and Li, 2000). However, there have been few systematic studies of these sensitization phenomena within the theoretical framework of existing kinetic models for quartz (Chen and Leung, 1998). The ability to make such a correction depends upon the assumption that electrons from the main OSL trap and from the trap responsible for the 110 °C TL peak use the same luminescence centers; this was suggested by Franklin et al. (1995) who compared the TL spectra of Scholefield et al. (1994) and the OSL spectrum obtained by Huntley et al. (1991). Polymeris et al. (2006) studied extensively the effects of annealing and irradiation treatments on the sensitivity and superlinearity properties of the 110 °C TL peak of 4 quartz samples.

The first part of this paper presents a simulation of the experimental data obtained by Wintle and Murray (1998) using particular thermal pretreatments; this simulation uses the comprehensive model developed by Bailey (2001). The complete experimental protocol of Wintle and Murray (1998) is simulated for both the natural and laboratory irradiated aliquots and includes the measurement of the sensitivity of the aliquots using the 110 °C TL peak. In the second part of the paper, an OSL pulse annealing procedure which uses different heating rates is simulated, for both a natural quartz aliquot and for an aliquot which is optically bleached and then irradiated in the laboratory.

## 2. Previous experimental and theoretical work on preheating

Wintle and Murray (1998) studied sensitivity changes that occurred during laboratory heating of a 30,000 yr old sedimentary quartz from Australia. They used two aliquots, one of which was in its natural state and the other which had been optically bleached and had subsequently received in the laboratory a dose of 56 Gy. The experiments consisted of preheating (holding at a temperature for 10 s) a single aliquot to progressively higher temperatures from 160 to 500 °C in increments of 10 °C and then measuring the OSL at 125 °C during a short 0.1 s stimulation. The 110 °C TL peak was measured at each step by delivering a small test dose of 0.1 Gy. The sensitivity, as measured by the 110 °C TL peak, of the natural sample was increased by ∼ 30% as the preheat temperature was increased from 160 to 300 °C (Fig. 7b of Wintle and Murray, 1998). The laboratory irradiated aliquot exhibited a much larger 110 °C TL peak sensitivity increase of ∼300% when the temperature was increased from 240 to 300 °C. Wintle and Murray (1998) also reported that the OSL signal increased with preheat temperature from 160 to 270 °C for the laboratory irradiated aliquots and decreased between 270 and 300 °C (Fig. 7a of Wintle and Murray, 1998). This decrease was due to the thermal emptying of the main OSL trap. The increase in OSL signal for the laboratory irradiated aliquot was previously believed to be associated with a thermal transfer phenomenon, moving electrons from shallow light-insensitive traps to the main OSL traps (Wintle and Murray, 1997). However, when Wintle and Murray (1998) used the 110 °C TL peak measurements to correct the OSL signals for change in sensitivity, the evidence for thermal transfer disappeared (Fig. 7c of Wintle and Murray, 1998).

Besides sensitivity change, trap emptying will also occur as higher temperatures are reached. Pulse annealing has been used to evaluate thermal activation energies and frequency factors for the traps that are emptied over the temperature range examined (e.g. Li and Chen, 2001). The technique of pulse annealing is similar, but not identical, to the experimental procedure used by Wintle and Murray (1998). Bailiff and Poolton (1991) describe "pulse annealing" measurements in feldspars, in which samples were subject to cycles of rapid heating to the selected temperature, cooling to RT and short measurements were made of the infrared stimulated luminescence (IRSL). Duller (1994) established a method of analysis using the percentage of IRSL signal remaining after pulse annealing potassium feldspars to successively higher temperatures. When the remaining IRSL was plotted as a function of temperature, a maximum value was obtained at ∼ 250 °C. This may be interpreted as representing the TL peak related to the electrons thermally ejected from the traps that are also able to be stimulated by IR; this TL peak is not normally seen because of the dominance of other TL peaks observed in a normal TL measurement.

Short and Tso (1994) described a way of evaluating thermal activation energies for electron traps in feldspars from the decreasing OSL intensity versus temperature plots using computer generated data within the general-one-trap (GOT) approximation. Huntley et al. (1996) described thermal detrapping of the fast OSL component in quartz, and from curve fitting of the decreasing OSL signal obtained the activation energy and frequency factor of the main OSL traps. Using the approach of Short and Tso (1994), Li et al. (1997) performed pulse annealing using different heating rates to reach the annealing temperature and used these data to evaluate the activation energy from the shift of the temperature at which the rate of reduction reaches a maximum for their K-feldspar. Bøtter-Jensen et al. (2003) point out that the interpretation of the plots of remaining OSL after a fixed time at various temperatures is complicated by the sensitivity change brought about by thermal treatment. From pulse-annealing curves obtained for quartz, Li and Chen (2001) showed that both the OSL reduction rate between 200 and 400 °C had a positive maximum and a negative minimum, both of which shifted with heating rate. Assuming first-order behavior, Li and Chen (2001) evaluated the trapping parameters from these curves and estimated the lifetime at 20 °C for the OSL trap and the reservoir. A further study of the thermal stability and pulse annealing in quartz was given by Li and Li (2006).

Recently, Pagonis and Chen (2007) simulated OSL pulse-annealing experiments using a simple kinetic model consisting of a trapping state, a recombination center and a hole reservoir. They showed numerical results in good qualitative agreement with the experimental results for quartz reported by Li and Chen (2001). However, the activation energies evaluated from simulation of the various heating rate measurements deviated in some cases from the values used in the simulation program and possible reasons for this deviation were discussed by Pagonis and Chen (2007).

## 3. Model and simulations

The simulations in this paper are carried out using the comprehensive quartz model developed by Bailey (2001). For easy reference, Fig. 1 shows the energy level diagram and the parameters used in the model based on empirical data are presented in Table 1. The model has been successful in simulating several TL and OSL phenomena in quartz (Bailey, 2001). Level 1 in the model represents the 110 °C TL shallow electron trap, which gives rise to a TL peak at ∼ 100 °C when measured with a heating rate of 5 K $s^{-1}$. This TL peak has been the subject of numerous studies because of its importance in predose dating (Bailiff, 1994) and retrospective dosimetry (Bailiff, 1997), as well as for its use in measuring the luminescence sensitivity (Stoneham and Stokes, 1991; Stokes, 1994; Murray and Roberts, 1998). Within the model, the 110 °C TL level is assigned a photostimulation probability since it has been shown to be light sensitive (Wintle and Murray, 1997). However, the corresponding OSL signal plays only a minor role in the current simulations, since OSL measurements are carried out at 125 °C. Level 2 represents a generic "230 °C TL level", typical of such TL peaks found in many sedimentary quartz samples. It is assumed that this TL trap is not light sensitive and thus it is not assigned a photostimulation probability. Levels 3 and 4 are usually termed the fast and medium OSL components (Bailey et al., 1997) and they yield TL peaks at ∼ 330 °C as well as giving rise to OSL signals. The photostimulation rates for these levels are discussed in some detail in the original paper by Bailey (2001). The model does not contain any of the slow OSL components which are known to be present in quartz (Singarayer and Bailey, 2003; Jain et al., 2003), and which were incorporated in later versions of the model (Bailey, 2004). The OSL signal simulated in the present work is measured during short stimulations of duration 0.1 s, and is therefore expected to be due almost entirely to the fast OSL component arising from level 3. Level 5 is a deep, thermally disconnected, electron center. Such a level is known to be necessary in order to explain several TL and OSL phenomena based on competition

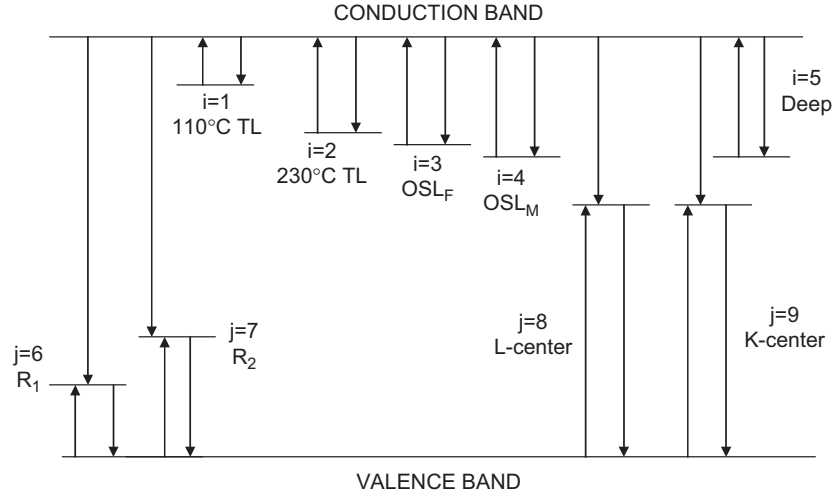


Fig. 1. Schematic diagram of the Bailey model (2001), consisting of a total of nine energy levels. The arrows indicate possible transitions.

Table 1
The Qtz-$A_1$ parameters of the original Bailey (2001) model

| Levels | | Parameters | | | | | | |
|---|---|---|---|---|---|---|---|---|
| | | $N_i$ ($cm^{-3}$) | $E_i$ (eV) | $s_i$ ($s^{-1}$) | $A_i$ ($cm^3\,s^{-1}$) | $B_i$ ($s^{-1}$) | $\theta_{0i}$ ($s^{-1}$) | $E_i^{th}$ (eV) |
| 1 | (110 °C TL) | 1.5e7 | 0.97 | 5e12 | 1e-8 | – | 0.75 | 0.1 |
| 2 | (230 °C TL) | 1e7 | 1.55 | 5e14 | 1e-8 | – | – | – |
| 3 | ($OSL_F$) | 1e9 | 1.7 | 5e13 | 1e-9 | – | 6 | 0.1 |
| 4 | ($OSL_M$) | 2.5e8 | 1.72 | 5e14 | 5e-10 | – | 4.5 | 0.13 |
| 5 | (Deep) | 5e10 | 2 | 1e10 | 1e-10 | – | – | – |
| 6 | ($R_1$-center) | 3e8 | 1.43 | 5e13 | 5e-7 | 5e-9 | – | – |
| 7 | ($R_2$-center) | 1e10 | 1.75 | 5e14 | 1e-9 | 5e-10 | – | – |
| 8 | (L-center) | 1e11 | 5 | 1e13 | 1e-9 | 1e-10 | – | – |
| 9 | (K-center) | 5e9 | 5 | 1e13 | 1e-10 | 1e-10 | – | – |

These parameters were used in all simulations described in this paper unless otherwise indicated in the text. $N_i$ are the concentrations of electron traps or hole centers, $s_i$ are the frequency factors, $E_i$ are the electron trap depths below the conduction band or hole center energy levels above the valence band, $A_i$ are the valence band to trap transition probability coefficients and $B_i$ are the conduction band to hole trap transition probability coefficients. The photo-eviction constants are $\theta_{0i}$ at $T = \infty$, and the thermal assistance energies are $E_i^{th}$.

between energy levels. The model contains also four hole trapping centers which act as recombination centers for optically or thermally released electrons. Levels 6 and 7 are thermally unstable, non-radiative recombination centers, similar to the "hole reservoirs" first introduced by Zimmerman (1971) in order to explain the predose sensitization phenomenon in quartz. Level 8 is a thermally stable, radiative recombination center termed the "luminescence center" (L in the Zimmerman model). Holes can be thermally transferred from the two hole reservoirs (levels 6 and 7) into the luminescence center via the valence band. Level 9 is a thermally stable, non-radiative recombination center termed a "killer" center (K in the Zimmerman model).

Adamiec et al. (2004, 2006) also presented a comprehensive kinetic model for the predose effects in quartz; it consisted of three non-radiative recombination centers and one radiative center, as well as two electron traps responsible for the 110 and 320 °C peaks, respectively, and a reservoir electron trap. The model successfully simulated the thermal activation characteristics and isothermal sensitization when the results were compared to experimental data.

In the current study, the computer code is written in *Mathematica*, and was tested for consistency by successfully reproducing several of the simulation results in Bailey (2001). The parameters are as defined by Bailey (2001); $N_i$ are the concentrations of electron traps or hole centers ($cm^{-3}$), $n_i$ are the concentrations of trapped electrons or holes ($cm^{-3}$), $s_i$ are the frequency factors (per second, $s^{-1}$), $E_i$ are the electron trap depths below the conduction band or hole center energy levels above the valence band (eV), $A_i$ are the valence band to trap transition probability coefficients ($cm^3\ s^{-1}$) and $B_i$ are the conduction band to hole center transition probability coefficients ($cm^3\ s^{-1}$). Other parameters related to the optically sensitive traps are the photo-eviction constant $\theta_{0i}$ ($s^{-1}$) at $T = \infty$, the thermal assistance energy $E_i^{\text{th}}$ (eV) and $P$ representing the photon stimulation flux. The parameters $n_c$ and $n_v$ represent the instantaneous concentrations of electrons and holes in the conduction and valence band correspondingly.

The equations used in this study are as follows:

$$\frac{dn_i}{dt} = n_c(N_i - n_i)A_i - n_i P\theta_{oi}e^{(-E_i^{\text{th}}/k_B T)} - n_i s_i e^{(-E_i/k_B T)} \quad (i = 1, \ldots, 5) \tag{1}$$

$$\frac{dn_j}{dt} = n_v(N_j - n_j)A_j - n_j s_j e^{(-E_j/k_B T)} - n_c n_j B_j \quad (j = 6, \ldots, 9) \tag{2}$$

$$\frac{dn_c}{dt} = R - \sum_{i=1}^{5}\left(\frac{dn_i}{dt}\right) - \sum_{j=6}^{9}(n_c n_j B_j), \tag{3}$$

$$\frac{dn_v}{dt} = \frac{dn_c}{dt} + \sum_{i=1}^{5}\left(\frac{dn_i}{dt}\right) - \sum_{j=6}^{9}\left(\frac{dn_j}{dt}\right). \tag{4}$$

The luminescence is defined as

$$L = n_c n_8 B_8 \eta(T) \tag{5}$$

with $\eta(T)$ representing the luminescence efficiency, and $R$ denoting the pair production rate (Bailey, 2001). The underlying assumption of Eq. (5) is that the OSL emission uses one radiative recombination center type.

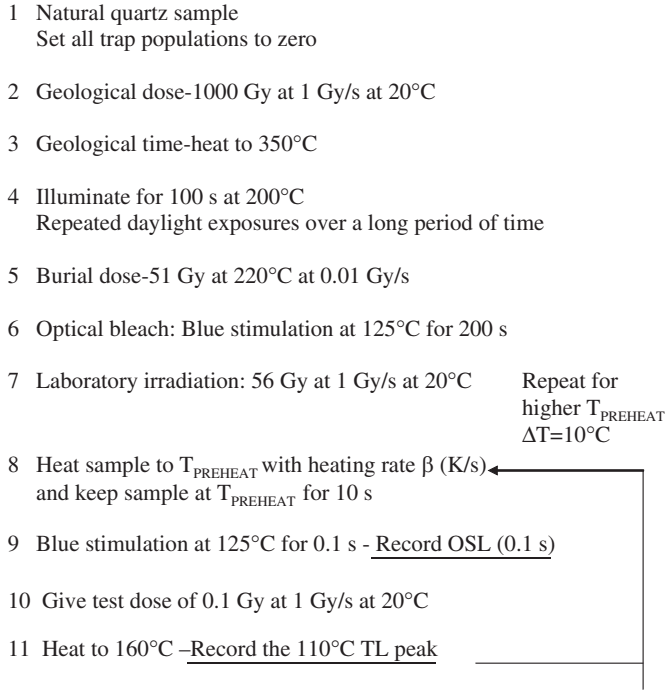


Fig. 2. The steps used in simulating the experimental procedure of Wintle and Murray (1998). The natural aliquot is simulated by omitting steps 6 and 7.

Fig. 2 shows the steps used in simulating the experimental procedure of Wintle and Murray (1998). The first 5 stages in Fig. 2 are identical to those employed by Bailey (2001, p. 24) to simulate the thermal and radiation history of a natural quartz sample. In step 1 all trap and center populations are set to zero. Step 2 represents the 1000 Gy geological dose received by the sample at 20 °C and with an irradiation rate of 1 Gy $s^{-1}$. In step 3 the sample is heated to 350 °C to simulate the effect of geological time, and step 4 (light exposure for 100 s at 200 °C) simulates repeated daylight exposure cycles over a long time period. The burial dose in step 5 is taken to be 51 Gy, close to the equivalent dose of the Australian quartz sample as measured by Wintle and Murray (1998). In both steps 4 and 5, the simulated bleaching and irradiations are simulated in such a way that the trap giving rise to the 110 °C TL peak (level 1) is kept empty, as indeed it is in nature. Steps 6 and 7 are used to simulate the laboratory bleached and irradiated aliquot used by Wintle and Murray (1998). In step 6 the OSL signal in the natural aliquot is bleached using blue light for 200 s at 125 °C. During step 7 the bleached aliquot is given a dose of 56 Gy at a rate of 1 Gy $s^{-1}$. In step 8 the aliquot is heated to a preheat temperature $T_{\text{PREHEAT}}$ with a heating rate of 1 K $s^{-1}$ and is kept at that temperature for 10 s. In step 9 a short optical stimulation of 0.1 s is delivered to the aliquot and the integrated OSL signal is recorded. In steps 10–11 the luminescence sensitivity is measured by delivering a test dose of 0.1 Gy, and subsequently heating the aliquot to 160 °C to measure the 110 °C TL peak. The process described in steps 8–11 is repeated for progressively higher preheat temperatures, in steps of 10 °C.

The simulation also contains additional stages not shown in Fig. 2, namely 1-second intervals of relaxation after each irradiation stage, as well as appropriate cooling-down periods after each heating stage in the simulation. The 1-second relaxation periods are necessary to allow the concentrations of electrons and holes in the conduction and valence band to drop to zero, before proceeding with the simulation.

The shape of the 110 °C TL peak remains constant during the simulations in this paper. The TL peak has the asymmetric shape expected for first-order kinetics. With the kinetic parameters $E$, $s$ used in the model the maximum intensity of the 110 °C peak obtained in steps 8 and 11 using a heating rate of 1 K s$^{-1}$ is located around 85 °C. The heating rate $\beta$ used in the simulation (steps 8 and 11 of Fig. 2 for the preheat and sensitivity simulations), does not affect the results of the simulation.

## 4. Results

### 4.1. The effect of the hole reservoirs on the OSL as a function of preheat temperature

We begin by investigating the importance of the two hole reservoirs (levels 6 and 7) in determining the shape of the OSL versus preheat temperature plots. The results of the simulation using four values of the parameter $N_6$ (namely $3\times10^7$, $3\times10^8$, $3\times10^9$ and $3\times10^{10}$ cm$^{-3}$) are shown in Fig. 3(a) for an aliquot that was optically bleached and given a dose of 56 Gy. The parameter $N_6$ represents the total concentration of available holes in the shallow reservoir $R_1$ (level 6 in Fig. 1), and the value used in the paper by Bailey (2001) was $N_6=3\times10^8$ cm$^{-3}$. The corresponding results of the simulation for a natural aliquot are shown in Fig. 3(c). Figs. 3(b) and (d) present the same data as Figs. 3(a) and (c), but normalized to the data point for the lowest available preheat temperature, in order to show the effect of parameter $N_6$ on the shape of the plots.

The results of Fig. 3(b) show that there are two possible behaviors of the OSL (0.1 s) signal as a function of the preheat temperature for the bleached and irradiated aliquot. For some values of the parameter $N_6$, the OSL stays constant for temperatures up to ∼ 220 °C and subsequently decreases continuously to zero as the temperature is increased to ∼ 320 °C. For other values of $N_6$, a peak is observed around 250 °C before the OSL drops to zero at higher temperatures. The corresponding normalized results for the natural sample are shown in Fig. 3(d), where an absence of any peak structure in the OSL versus temperature plots is noted for all values of $N_6$. These results are presented in more detail in Figs. 4 and 5 and are discussed in subsequent sections.

The results of Figs. 3(a) and (c) are perhaps surprising at first glance; they show that, as the concentration $N_6$ is increased, the OSL signal decreases. This behavior can be explained by the fact that the shallow reservoir $R_1$ (level 6) is acting in direct competition with the luminescence center L (level 8) for the capture of holes from the valence band during the irradiation of the sample. As $N_6$ increases, the number of holes captured in level 6 during irradiation increases, causing less holes to be trapped in the luminescence center L (level 8). This in turn causes a decrease of the measured OSL signal which is

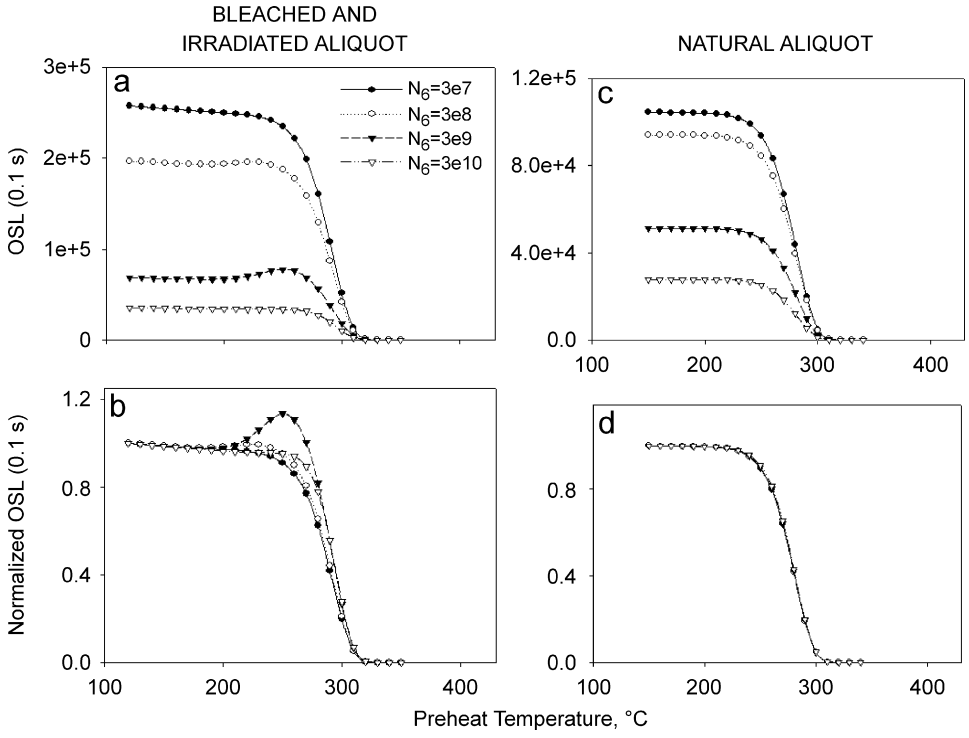


Fig. 3. The results of the simulation shown in Fig. 2 when using different values of the parameter $N_6$ in the model. $N_6$ represents the total concentration of holes in the shallow reservoir $R_1$. Figs. (a) and (c) are for an aliquot that was bleached and irradiated with 56 Gy and figures (b) and (d) are for a natural aliquot. Figures (c) and (d) show the same data as (a) and (b) but normalized to the data point for the lowest preheat temperature.

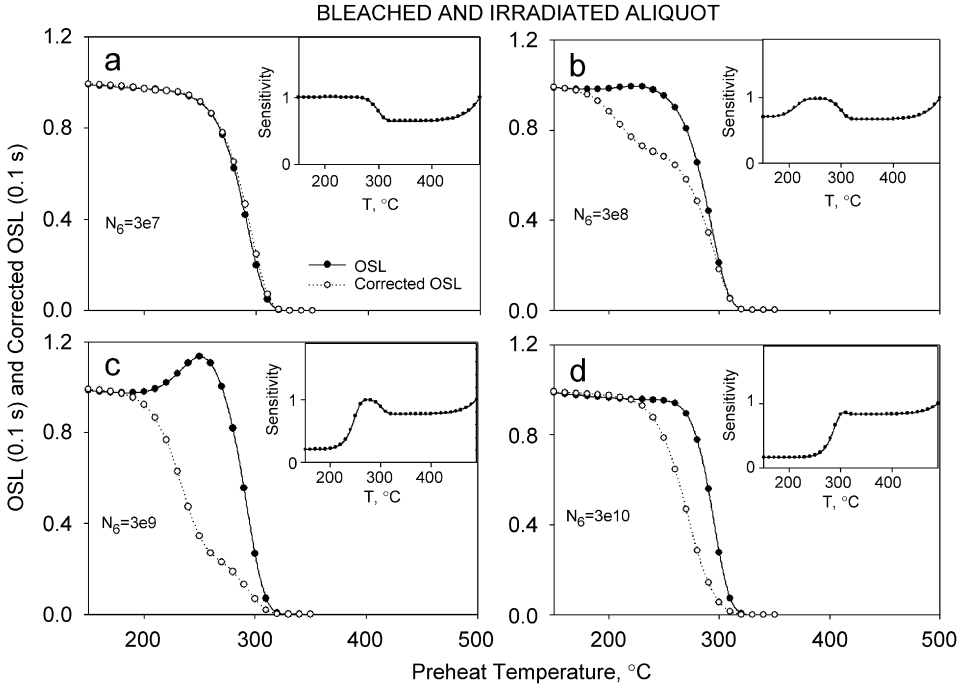


Fig. 4. Results of the simulation shown in Fig. 2 for a bleached and irradiated aliquot obtained using four values of the parameter $N_6$. The open circles represent the sensitivity-corrected OSL signal and the filled circles are the uncorrected OSL data. The insets show the 110 °C TL peak sensitivity normalized to the value measured for the 500 °C preheat.

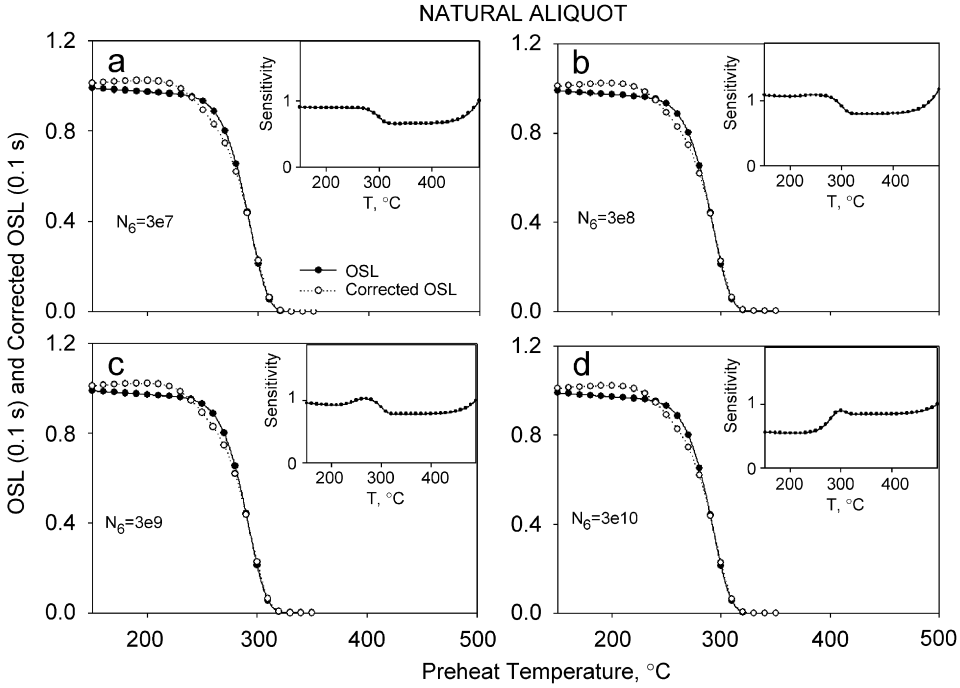


Fig. 5. As in Fig. 4, but for the natural aliquot.

proportional to the concentration $n_8$, the concentration of holes in level 8, as shown in Eq. (5).

The behavior shown in Fig. 3 is similar to the simulation results obtained by Pagonis and Chen (2007) using their much simpler model. They investigated two cases depending on whether their hole reservoir was part of the model or not. A peak in the OSL versus preheat temperature plot was associated with the presence of the hole reservoir in their model. The peak for $N_6 = 3 \times 10^9\,\mathrm{cm}^{-3}$ (Fig. 3(b)) is similar to the experimental data of Wintle and Murray (1998) as shown in Fig. 6 (Fig. 7(a) of Wintle and Murray, 1998). The simulated output for $N_6 = 3 \times 10^8\,\mathrm{cm}^{-3}$ as used by Bailey (2001)

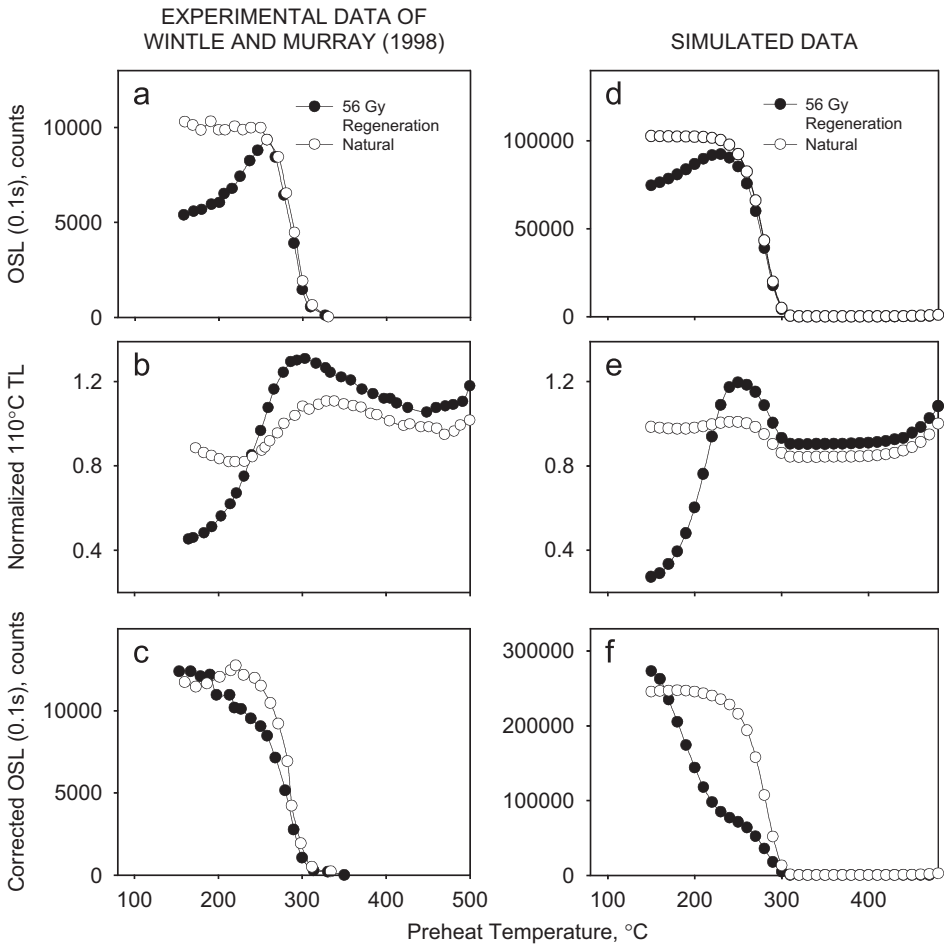


Fig. 6. A comparison of the experimental data of Wintle and Murray (1998) (a), (b) and (c) and the results of the simulations (d), (e) and (f). The simulated OSL signals and sensitivity-corrected signals were multiplied by appropriate scaling factors to aid comparison.

produces a scarcely perceptible rise in OSL signal at about 250 °C (Figs. 3(a) and (b)). Although it may be possible to get quantitative agreement between the results of the simulations (e.g. in Fig. 3(a)) and the experimental data of Wintle and Murray (1998) in Fig. 6(a) by adjusting the parameters in the Bailey model, we prefer to leave the parameters unchanged and to focus instead on drawing more general qualitative conclusions about the various processes taking place.

### *4.2. Sensitivity correction of the OSL (0.1 s) signals for bleached and irradiated aliquots*

Fig. 4 shows the results of the simulation steps in Fig. 2 for the bleached and irradiated aliquot. Figs. 4(a)–(d) correspond to four values of the parameter $N_6$, namely $3 \times 10^7$, $3 \times 10^8$, $3 \times 10^9$ and $3 \times 10^{10}\,\mathrm{cm}^{-3}$, previously displayed in Figs. 3(a) and (b). The insets of Fig. 4 show the simulated change in the sensitivity of the 110 °C TL peak to a test dose of 0.1 Gy (steps 10–11 in Fig. 2); these sensitivities are normalized using the value for 500 °C.

Consideration of Figs. 4(a)–(d) indicates several interesting trends. Firstly, the exact form of the response depends critically on the value of $N_6$, the concentration of holes in the Zimmerman reservoir $R_1$ used in the Bailey (2001) model (level 6 in Fig. 1). Secondly, the prominent peaks appearing in the uncorrected OSL data (filled circles) in Figs. 4(b) and (c) around 250 °C, disappear after the OSL data is corrected (open circles) using the corresponding sensitivity values. This output verifies the assumption of Wintle and Murray (1998) that these peaks are due to sensitivity changes occurring during the heating, rather than being due to thermal transfer processes, as was assumed earlier by Wintle and Murray (1997). After the sensitivity correction is carried out, a small shoulder remains in Figs. 4(b) and (c) around 260 °C; this is followed by a gradual decline in OSL to zero at higher temperatures. This shoulder can be seen in both the experimental data of Wintle and Murray (1998) and in the simulation results (Fig. 6); this feature of the data is explained in Section 4.4.

Thirdly, the insets of Figs. 4(a)–(d) show that the sensitivity changes over the range from 160 to 500 °C by factors of −40%, +50%, +450% and +500% as the value of $N_6$ is increased. This increase of the sensitivity as the parameter $N_6$ is increased can be understood within the model as follows. As $N_6$ increases, one would expect more holes to be trapped into the Zimmerman reservoir $R_1$ during irradiation of the sample. This larger concentration of holes in $R_1$ will result in a larger

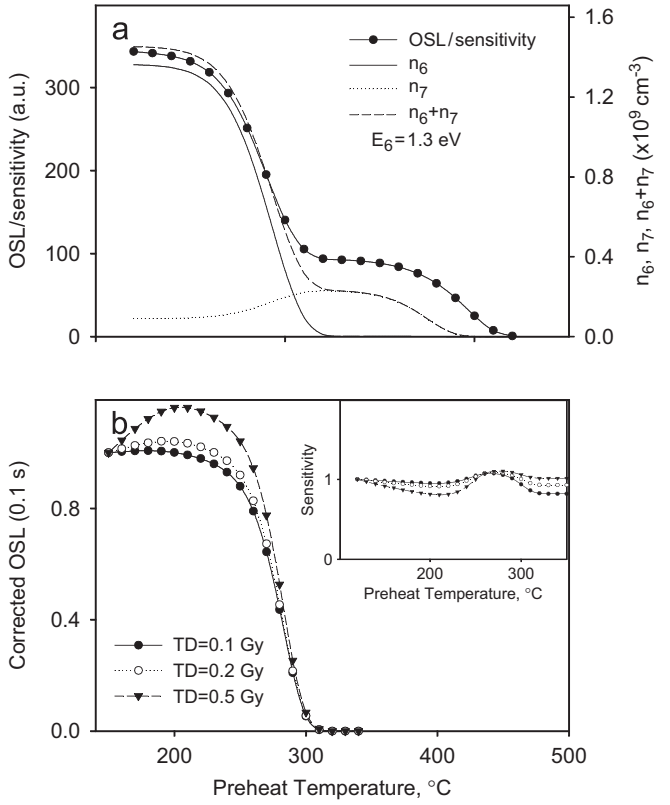


Fig. 7. (a) Simulation of the effect of the parameter $E_6$ on the shape of the OSL vs. Preheat temperature graph. (b) Simulation of the effect of the size of the test dose (TD) on the increase of the sensitivity-corrected OSL signal with preheat temperature. The inset of Fig. 7(b) shows the corresponding change in the normalized sensitivity of the quartz samples in this temperature region.

number of holes being transferred from $R_1$ into the luminescence center L during the preheating of the sample, and will lead to a larger increase in the sensitivity of the sample. The peak in sensitivity shown in the inset of Fig. 4(c) is in reasonably close agreement, and of the same order of magnitude ($\sim$ 400%), as the experimental results of Wintle and Murray (1998) (Fig. 6(b)).

A fourth observation from the simulations in Figs. 4(b)–(d) is that the sensitization (shown in the insets) reaches its maximum at a temperature of $\sim$ 280 °C, signaling the end of the sensitization process. The mechanism behind this result is shown in more detail in Fig. 7 and is discussed in Section 4.5. The sensitivity remains fairly constant at temperatures higher than $\sim$ 280 °C and reaches an equilibrium value. However, at a temperature of $\sim$ 310 °C the OSL decreases due to the effective emptying of the main OSL traps (level 3).

### 4.3. Sensitivity correction of the OSL (0.1 s) signals for natural aliquots

The results of the simulations for a natural quartz sample are shown in Fig. 5 for the same values of $N_6$, namely $3 \times 10^7$–$3 \times 10^{10}$ cm$^{-3}$.

Firstly, it can be seen that the different values of $N_6$ seem to have no effect on the shapes of either the uncorrected or the corrected OSL signal and there is an absence of any peak at $\sim$ 250 °C. Both these observations can be understood by the fact that in the natural sample one would expect the shallow hole reservoir $R_1$ to have been thermally activated during the burial period of the sample. This is equivalent to step 5 of the simulation in Fig. 2, in which the burial dose of 51 Gy is assumed to be delivered at a temperature of 220 °C (as discussed in Section 3); this temperature is high enough to thermally transfer holes from the shallow hole reservoir $R_1$ (level 6) to the luminescence center L (level 8) during the natural burial period, but not high enough to thermally empty the deeper hole reservoir $R_2$ (level 7).

Secondly, as the concentration of hole centers $N_6$ is changed, the sensitivity changes for the natural aliquot always remains much smaller than the changes for the bleached and irradiated aliquot (Fig. 4). More specifically the data shown in the insets of Figs. 5(a)–(d) show that the sensitivity changes for the natural aliquots are only of the order of 20–30%. The dramatic difference in sensitivity changes between the natural aliquot (Fig. 5) and the bleached and irradiated aliquot (Fig. 4) is directly attributable to the thermal activation of the hole reservoir $R_1$ for the natural sample, in agreement with the findings and interpretation given by Wintle and Murray (1998).

We also note that there is a slight increase in the corrected OSL signal (open circles) at low preheat temperatures, up to $\sim$ 220 °C (Fig. 5). This feature is also shown in the experimental data (Fig. 7(c) of Wintle and Murray, 1998) which are shown in Fig. 6(c).

### 4.4. Direct comparison of the simulation results with the experimental data

Murray and Wintle (1999) performed an isothermal decay study of their sample (WIDG8) and obtained the following values for the kinetic parameters for the main OSL traps: for the fast OSL component $E_3 = 1.66 \pm 0.03$ eV, $s_3 = 10^{13}$ s$^{-1}$ and $E_4 = 1.75 \pm 0.15$ eV, $s_4 = 10^{13}$ s$^{-1}$ for the medium OSL component (Components A and C in their Table 2, p. 124). They also identified a second thermally unstable OSL signal (component B) with kinetic parameters $E = 1.14$ eV, $s = 10^{10}$ s$^{-1}$. From the sensitivity changes for the same sample they found the following values for the parameters of the hole reservoirs: $E_6 = 0.95 \pm 0.17$ eV, $s_6 = 10^8$ s$^{-1}$ and $E_7 = 1.26 \pm 0.10$ eV and $s_7 = 10^{10}$ s$^{-1}$ (components B and A respectively in their Table 1).

Fig. 6 shows a side-by-side comparison of the experimental data of Wintle and Murray (1998, their Figs. 7(a)–(c)) with the results of our simulation. Figs. 6(a)–(c) show the redrawn data of Wintle and Murray (1998) and Figs. 6(d)–f the corresponding results of the simulation. The latter were obtained using the following, slightly adjusted, values for the kinetic parameters: $E_3 = 1.59$ eV, $s_3 = 10^{13}$ s$^{-1}$, $E_4 = 1.72$ eV, $s_4 = 10^{13}$ s$^{-1}$, $E_6 = 0.82$ eV, $s_6 = 10^8$ s$^{-1}$, $E_7 = 1.29$ eV and $s_7 = 10^{10}$ s$^{-1}$ and $N_6 = 3 \times 10^9$ cm$^{-3}$ for the total concentration of the shallow reservoir $R_1$. The rest of the parameters are identical to the

original Bailey (2001) parameters. Our value of $E_6 = 0.82$ eV is within the broad experimental limits of $E_6 = 0.95 \pm 0.17$ eV established by Wintle and Murray (1999).

We emphasize that our goal here is not to provide an exact quantitative agreement between theory and experiment, but rather to demonstrate that the Bailey model can help us understand several unusual and previously unexplained features of the experimental data. It should be noted that in experimental studies (e.g. Wintle and Murray, 1998, 1999), the OSL signals are derived from aliquots made up of several thousand grains. OSL measurements of single quartz grains show that the individual grains exhibit a wide range of behavior (e.g. Adamiec, 2000; Yoshida et al., 2000). Thus, although experimental results obtained on one aliquot can be used to characterize the average OSL behavior of the grains making up that aliquot, there may be differences for other aliquots that are made up of a different selection of grains. However, determinations of parameters made using measurements utilizing many aliquots suggest that an average behavior for that sample can be assumed.

In Figs. 6(a) and (d) the OSL signal of the bleached and irradiated aliquot (filled circles) is seen to increase up to a temperature of 240 °C and to subsequently decrease to zero at a temperature of ∼ 310 °C. The increase of OSL with the preheat temperature can be explained within the Bailey model as follows: as the preheat temperature increases, more holes are transferred from $R_1$ to $R_2$ into the luminescence center and this leads to an increase of the sensitivity according to Eq. (5). The corresponding data in Figs. 6(a) and (d) for the natural aliquot (open circles) does not show this initial increase of OSL with preheat temperature. As discussed earlier, this is due to the fact that the shallow reservoir $R_1$ (level 6) was already thermally activated during the burial history of the sample.

The Bailey model can also be used to provide an explanation of the shoulder between ∼ 200 and 260 °C (Figs. 6(c) and (f)) for the bleached and irradiated aliquot (filled circles). This shoulder is much more prominent in the simulated data (Fig. 6(f)) than in the experimental data (Fig. 6(c)). By varying the parameters in the model, it is possible to identify the cause of this shoulder. As shown in Fig. 7(a), the shoulder becomes more prominent when the activation energy for the reservoir $R_1$ is changed from the original value of $E_6 = 1.43$ eV to a slightly smaller value of $E_6 = 1.3$ eV. Examination of the results of the simulations in Fig. 7(a) shows that the charge in reservoir $R_1$ ($n_6$) is emptied thermally by 220 °C (solid line). Between 150 and 220 °C, the population in the second hole reservoir $R_2$ ($n_7$) increases. Between 220 and 260 °C the combined concentrations $n_6$ and $n_7$ are constant. Above 260 °C $R_2$ is thermally emptied and $n_7$ decreases to zero. These results show that the apparent shoulders and remaining small plateaus in Figs. 4(b) and (c) (filled circles) are not due to thermal transfer phenomena from shallow traps, but rather are caused by the fact that the thermal emptying of the hole reservoirs $R_1$ and $R_2$ occurs at different temperatures.

Fig. 6(c) shows that the OSL signal for the natural aliquot initially increases slightly between 150 and 220 °C (open circles). This initial increase could be interpreted as a thermal transfer of charge from shallower traps into the main OSL trap, the fast component. However, examination of the results of the simulations shows that this effect is caused instead by the successive irradiations with the test dose of 0.1 Gy. The effect of the repeated test dose on the OSL as a function of preheat temperature is shown in Fig. 7(b). The inset of Fig. 7(b) shows the corresponding change in the normalized sensitivity of the quartz samples in this temperature region. As successive test doses (TD) are delivered to the natural aliquot, holes created by irradiation in the valence band get captured in the shallow reservoir $R_1$ (level 6); thus the concentration of holes $n_6$ in level 6 increases with each successive test dose delivery, as shown in Fig. 7(b) for different TD. When these holes are thermally transferred to the luminescence center, they lead to an increase in the measured sensitivity between 150 and 220 °C (inset of Fig. 7(b)) and the OSL signal increases in this region (Fig. 7(b)).

### 4.5. Thermal transfer mechanism for the Zimmerman reservoirs

The change in concentrations of holes ($n_6$ and $n_7$) in the Zimmerman reservoirs $R_1$ and $R_2$, respectively, with preheat temperature are shown in Fig. 8(a) for the bleached and irradiated aliquot and for the natural aliquot in Fig. 8(b). As might be expected, the model shows that as the preheat temperature is increased, the concentrations of holes in the reservoirs $n_6$ and $n_7$ decrease to zero, while the concentration $n_8$ of holes in the luminescence center L is increased. This is in agreement with the original mechanism proposed by Zimmerman (1971), in which a thermal transfer of holes takes place from $R_1$ and $R_2$ into L. The thermal transfer of holes is complete at ∼ 280 °C for both $R_1$ and $R_2$, in agreement with the results for the sensitivity maximum shown in the insets of Figs. 4 and 5.

It is noted that additional experimental work on quartz has been carried out using very high temperature annealing. Bøtter-Jensen et al. (1995) studied the effect of high temperature annealing on quartz OSL signals and found dramatic changes in the range 500–800 °C. They modeled these dramatic sensitivity changes by assuming the existence of two types of recombination centers, a radiative and a non-radiative type. In their model, high temperature annealing either removed non-radiative recombination centers, or created additional radiative recombination centers, leading to increased sensitivity. This model is clearly more complex than the simpler model presented in this paper.

For the bleached and irradiated aliquot $n_6 \gg n_7$ at low temperatures (Fig. 8(a)), while for the natural aliquot $n_6 \sim n_7$ (Fig. 8(b)). The small peak in $n_7$ as a function of preheat temperature (Fig. 8(a)) is interpreted as being due to the recapture of holes previously released from $R_1$ into the thermally more stable reservoir $R_2$ when preheating at temperatures between 200 and ∼ 250 °C.

The change in the combined hole concentrations ($n_6 + n_7$) is $\sim 1.4 \times 10^9\ \mathrm{cm}^{-3}$ (Fig. 8(a)). The concentration of holes in the luminescence center $n_8$ changes by almost exactly the

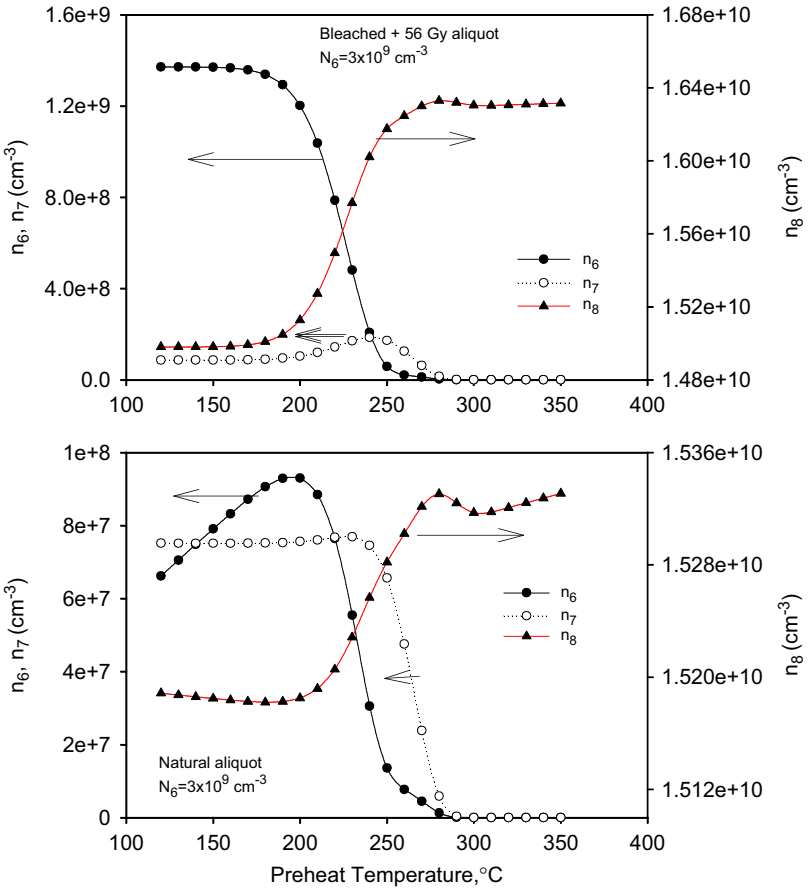


Fig. 8. The mechanism of hole transfer from $R_1$ and $R_2$ into the luminescence center L during the experiment for (a) the bleached and irradiated aliquot and (b) the natural aliquot.

same amount, as seen from the data in Fig. 8(a) (right-hand axis). This indicates that almost 100% of the holes stored in the reservoirs ($R_1$ and $R_2$) are transferred to the luminescence center L. Complete thermal transfer and hole conservation is also seen for the natural sample (Fig. 8(b)).

### *4.6. Simulation of the pulse annealing experiments using variable heating rates*

We have also simulated OSL measured in pulse annealing experiments that use different heating rates, as reported previously by Duller (1994) for potassium feldspar and by Li and Chen (2001) for quartz. Li and Chen (2001) reported a peak in the plot of the pulse-annealed OSL as a function of preheat temperature and they interpreted this as being due to the thermal transfer of holes from a single reservoir into the recombination center (as per Zimmerman, 1971), contributing to an increase in the sensitivity. When the reduction in OSL signal between consecutive measurements was plotted as a function of temperature, a minimum was seen at $\sim 280\,^{\circ}C$ for the bleached and irradiated aliquot and a maximum at $\sim 330\,^{\circ}C$ for both aliquots (Fig. 2 of Li and Chen, 2001). Each point is associated with the inflection point in the original plot of the OSL signal as a function of annealing temperature for a given heating rate. Li and Chen (2001) assumed that both the transfer of holes from the reservoir and the recombination process can be approximated by first-order kinetics; they used the positions of these (negative and positive) peaks and the related heating rate to evaluate the activation energies and frequency factors of the two processes giving rise to these peaks.

The steps followed in the pulse annealing technique of Li and Chen (2001) are identical to those used by Wintle and Murray (1998) shown in Fig. 2 of this paper, with one experimental difference. The latter authors kept their sample at the preheat temperature for 10 s and subsequently cooled it to room temperature at an unknown cooling rate, while the former authors heated their sample and immediately cooled it to room temperature at a high cooling rate. We have run the simulations for both these experimental procedures and found no difference between the simulation results.

The results of simulating the pulse annealing technique of Li and Chen (2001) for a natural aliquot and for a bleached and irradiated aliquot are shown in Figs. 9 and 10, respectively. The heating rates used were 0.5, 1, 2 and $3\,K\,s^{-1}$ and the steps of the pulse annealing were of $\Delta T = 10\,^{\circ}C$ as in the experiments of Li and Chen (2001). The OSL reduction rate plots yield peaks for the bleached and irradiated aliquot which shift to higher temperatures with increasing heating rates (Figs. 9(b) and (b)).

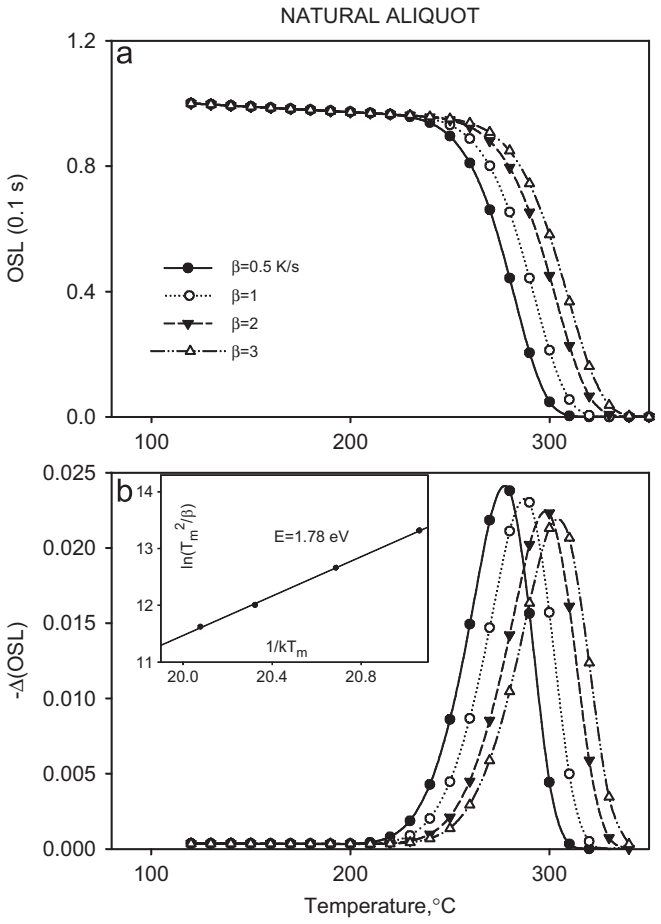


Fig. 9. OSL simulation results of pulse annealing of a natural aliquot. (a) Pulse annealing carried out using either 0 or 10 s at the applied preheat temperature when four different heating rates ($\beta$) are used. (b) Data ($-\Delta$(OSL)), the difference between consecutive measurements in (a) plotted as a function of the same preheat temperature.

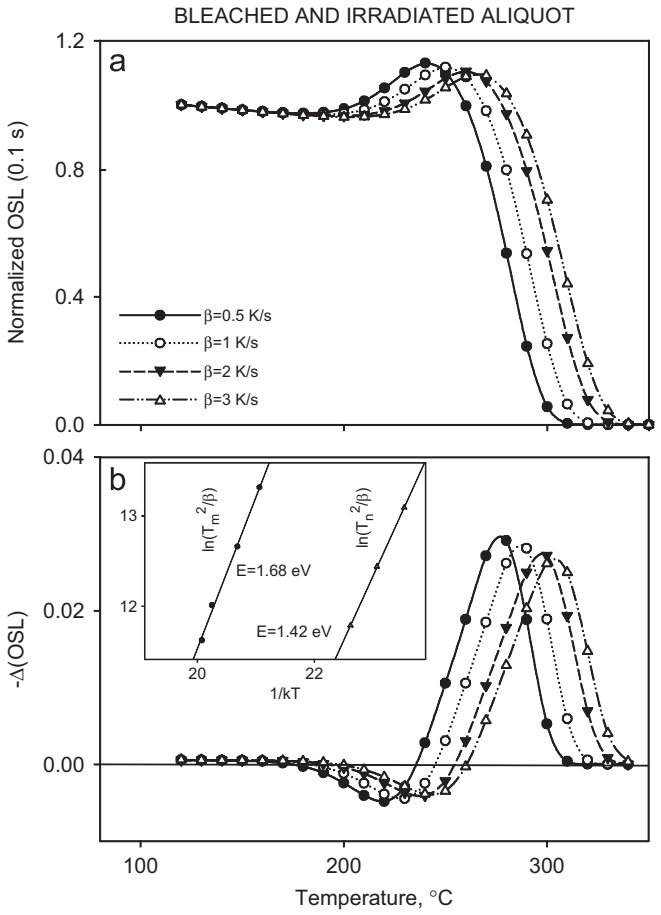


Fig. 10. Same as Fig. 9, but for a bleached and irradiated aliquot.

Assuming first-order kinetics, the relationship between $E$, $s$, the maximum temperature $T_m$ and the heating rate $\beta$ is

$$\frac{\beta E}{kT_m^2} = s \exp\left(-\frac{E}{kT_m}\right). \quad (6)$$

This equation is regularly used to obtain $E$ and $s$ values for TL peaks (Chen and McKeever, 1997). However, Li et al. (1997) showed that the same equation was valid for the peaks obtained using pulse annealing data for OSL signals. According to Eq. (6), a plot of ln $(T_m^2/\beta)$ as a function of $1/kT_m$ is expected to yield a straight line as shown in the inset in Fig. 9(b). From its slope $E$, the activation energy, can be evaluated. The natural aliquot yields a straight line (Fig. 9), with a slope of $E = 1.78 \pm 0.02$ eV; this can be compared with the value of $E_3 = 1.70$ eV used in the Bailey model for the main OSL traps (a difference of 5%). Using the $y$-intercept of the inset in Fig. 9(b), we estimate the corresponding value of the frequency factor to be $s_3 = 7 \times 10^{14}$ s$^{-1}$, which compares reasonably well with the value of $s_3 = 5 \times 10^{13}$ s$^{-1}$ used in the model.

For the bleached and irradiated aliquot, the OSL is simulated using the same set of heating rates, and the equivalent results are shown in Figs. 10(a) and (b). Both the maximum between 280 and 310 °C and the minimum at ~ 250 °C shift to higher temperatures with higher heating rates, as in the experimental results reported by Li and Chen (2001). Results for the maximum $T_m$ yield a straight line with a slope $E = 1.68 \pm 0.07$ eV as compared to $E_3 = 1.70$ eV used in the model, a 1% difference in the activation energy $E$. Using the $y$-intercept of the inset in Fig. 10(b) the corresponding frequency factor was $s_3 = 8 \times 10^{13}$ s$^{-1}$, which compares well with the value of $s_3 = 5 \times 10^{13}$ s$^{-1}$ used in the model. The inset of Fig. 10(b), shows $\ln(T_n^2/\beta)$ plotted against $1/(kT_n)$ where $T_n$ is the minimum temperature, and the best straight line yields a slope of $1.42 \pm 0.02$ eV as compared to the value of $E_6 = 1.43$ eV entered into the simulation for the hole reservoir $R_1$. This represents an error of only 0.6% in the activation energy. Using the $y$-intercept of the inset in Fig. 10(b) the corresponding value of the frequency factor was $s_6 = 1.2 \times 10^{13}$ s$^{-1}$, which compares well with the value of $s_6 = 5 \times 10^{13}$ s$^{-1}$ used in the model. It is noted that, though the original values of $E$ in the model ($E_3 = 1.70$ eVand $E_6 = 1.43$ eV) are within the standard deviation of the values of $E$ obtained by analysis of the simulation data, they are not identical; however, they are within 1–5%. This is to be expected because of the numerical approximations made during the numerical integration of the eleven differential equations.

The results obtained in these simulations support the assertion made by Li and Chen (2001) that both the minimum and the maximum peaks in these types of plots result from first-order kinetic processes; thus, a method that uses a variable heating rate can be expected to yield the correct activation energies and frequency factors, and hence, correct lifetimes.

Pagonis and Chen (2007) studied the effect of non-first-order kinetics on the values of the kinetic parameters obtained from the pulse annealing technique in their simple three-level model. They changed the retrapping probability by three orders of magnitude, but the plot of $\ln(T_m^2/\beta)$ versus $1/(kT_m)$ was still linear. However, the activation energies differed by as much as 25% from the values of the parameters in the model. Pagonis and Chen (2007) discussed in some detail the consequences of these deviations for the expected lifetimes of the OSL traps at room temperature.

## 5. Conclusions

Bailey's (2001) model can be used to simulate the experimental procedure used during OSL pulse annealing studies. With only minor changes in the kinetic parameters, the model produced the correct dependence of the OSL signal on the preheat temperature, as found in published experimental studies (Wintle and Murray, 1998), even extending to preheat temperatures of 500 °C. It was also shown that the pulse annealing curves previously discussed by Duller (1994) for potassium feldspar and by Li and Chen (2001) for quartz, can also be simulated using the Bailey (2001) model. The results of the simulations show that the activation energies and frequency factors were retrievable using OSL measurements made with a variable heating rate provided retrapping was relatively low. These values support the claims that the evaluated lifetimes at ambient temperature are reliable.

## References


Adamiec, G., 2000. Variations in luminescence properties of single quartz grains and their consequences for equivalent dose estimation. Radiat. Meas. 32, 427–432.

Adamiec, G., Garcia-Talavera, M., Bailey, R.M., Iniguez de la Torre, P., 2004. Application of a genetic algorithm to finding parameter values for numerical stimulation of quartz luminescence. Geochronometria 23, 9–14.

Adamiec, G., Bluszcz, A., Bailey, R., Garcia-Talavera, M., 2006. Finding model parameters: genetic algorithms and the numerical modelling of quartz luminescence. Radiat. Meas. 41, 897–902.

Bailey, R.M., 2001. Towards a general kinetic model for optically and thermally stimulated luminescence of quartz. Radiat. Meas. 33, 17–45.

Bailey, R.M., 2004. Paper I—simulation of dose absorption in quartz over geological timescales and its implications for the precision and accuracy of optical dating. Radiat. Meas. 38, 299–310.

Bailey, R.M., Smith, B.W., Rhodes, E.J., 1997. Partial bleaching and the decay form characteristics of quartz OSL. Radiat. Meas. 27, 123–136.

Bailiff, I.K., 1994. The pre-dose technique. Radiat. Meas. 23, 471–479.

Bailiff, I.K., 1997. Retrospective dosimetry with ceramics. Radiat. Meas. 27, 923–941.

Bailiff, I.K., Poolton, N.R.J., 1991. Studies of charge transfer mechanisms in feldspars. Nucl. Tracks Radiat. Meas. 18, 111–118.

Bøtter-Jensen, L., Agersnap Larsen, N., Mejdahl, V., Poolton, N.R.J., Morris, M.F., McKeever, S.W.S., 1995. Luminescence sensitivity changes in quartz as a result of annealing. Radiat. Meas. 24, 535–541.

Bøtter-Jensen, L., McKeever, S.W.S., Wintle, A.G., 2003. Optically Stimulated Luminescence Dosimetry. Elsevier, Amsterdam.

Bulur, E., Bøtter-Jensen, L., Murray, A.S., 2000. Optically stimulated luminescence from quartz measured using the linear modulation technique. Radiat. Meas. 32, 407–411.

Chen, G., Li, S.H., 2000. Studies of quartz 110 °C thermoluminescence peak sensitivity change and its relevance to OSL dating. J. Phys. D 33, 437–443.

Chen, G., Li, S.H., Murray, A.S., 2000. Study of 110 °C TL peak sensitivity in optical dating of quartz. Radiat. Meas. 31, 641–645.

Chen, R., Leung, P.L., 1998. Processes of sensitization of thermoluminescence in insulators. J. Phys. D 31, 2628–2635.

Chen, R., McKeever, S.W.S., 1997. Theory of Thermoluminescence and Related Phenomena. World Scientific, Singapore.

Duller, G.A.T., 1994. A new method for the analysis of infrared stimulated luminescence data from potassium feldspars. Radiat. Meas. 23, 281–285.

Franklin, A.D., Prescott, J.R., Scholefield, R.B., 1995. The mechanism of thermoluminescence in an Australian sedimentary quartz. J. Lumin. 63, 317–326.

Huntley, D.J., Godfrey-Smith, D.I., Haskell, E.H., 1991. Light-induced emission spectra from some quartz and feldspars. Nucl. Tracks Radiat. Meas. 18, 127–131.

Huntley, D.J., Short, M.A., Dunphy, K., 1996. Deep traps in quartz and their use for optical dating. Can. J. Phys. 74, 81–91.

Jain, M., Murray, A.S., Bøtter-Jensen, L., 2003. Characterisation of blue-light stimulated luminescence components in different quartz samples: implications for dose measurement. Radiat. Meas. 37, 441–449.

Li, B., Li, S.-H., 2006. Studies of thermal stability of charges associated with thermal transfer of OSL from quartz. J. Phys. D 39, 2941–2949.

Li, B., Li, S.H., Wintle, A.G., 2006. Observations of thermal transfer and the slow component of OSL signals from quartz. Radiat. Meas. 41, 639–648.

Li, S.-H., Chen, G., 2001. Studies of thermal stability of trapped charges associated with OSL from quartz. J. Phys. D 34, 493–498.

Li, S.-H., Tso, M.Y.W., Wong, N.W., 1997. Parameters of OSL traps determined with various heating rates. Radiat. Meas. 27, 43–47.

Murray, A.S., Roberts, R.G., 1998. Measurement of the equivalent dose in quartz using a regenerative-dose single-aliquot protocol. Radiat. Meas. 29, 503–515.

Murray, A.S., Wintle, A.G., 1999. Isothermal decay of optically stimulated luminescence in quartz. Radiat. Meas. 30, 119–125.

Murray, A.S., Wintle, A.G., 2000. Luminescence dating of quartz using an improved single-aliquot regenerative-dose protocol. Radiat. Meas. 32, 57–73.

Pagonis, V., Chen, R., 2007. Simulation of OSL pulse-annealing at different heating rates: conclusions concerning the evaluated trapping parameters and lifetimes. Geochronometria, submitted for publication.

Polymeris, G., Kitis, G., Pagonis, V., 2006. The effects of annealing and irradiation on the sensitivity and superlinearity properties of the 110 °C thermoluminescence peak of quartz. Radiat. Meas. 41, 554–564.

Rhodes, E.J., 1988. Methodological considerations in the optical dating of quartz. Quat. Sci. Rev. 7, 395–400.

Scholefield, R.B., Prescott, J.R., Franklin, A.D., Fox, P.J., 1994. Observations on some thermoluminescence emission centers in geological quartz. Radiat. Meas. 23, 409–412.

Short, M.A., Tso, M.Y.W., 1994. New methods for determining the thermal activation energies of light sensitive traps. Radiat. Meas. 23, 335–338.

Singarayer, J.S., Bailey, R.M., 2003. Further investigations of the quartz optically stimulated luminescence components using linear modulation. Radiat. Meas. 37, 451–458.

Stokes, S., 1994. The timing of OSL sensitivity changes in a natural quartz. Radiat. Meas. 23, 601–606.

Stoneham, D., Stokes, S., 1991. An investigation of the relationship between the 110 °C TL peak and optically stimulated luminescence in sedimentary quartz. Nucl. Tracks Radiat. Meas. 18, 119–123.

Wintle, A.G., Murray, A.S., 1997. The relationship between quartz thermoluminescence, photo-transferred thermoluminescence and optically stimulated luminescence. Radiat. Meas. 27, 611–624.

Wintle, A.G., Murray, A.S., 1998. Towards the development of a preheat procedure for OSL dating of quartz. Radiat. Meas. 29, 81–94.

Wintle, A.G., Murray, A.S., 1999. Luminescence sensitivity changes in quartz. Radiat. Meas. 30, 117–118.

Wintle, A.G., Murray, A.S., 2006. A review of quartz optically stimulated luminescence characteristics and their relevance in single aliquot regeneration dating protocols. Radiat. Meas. 41, 369–391.

Yoshida, H., Roberts, R.G., Olley, J.M., Laslett, G.M., Galbraith, R.F., 2000. Extending the age range of optical dating using single 'supergrains' of quartz. Radiat. Meas. 32, 439–446.

Zimmerman, J., 1971. The radiation-induced increase of the 100 °C thermoluminescence sensitivity of fired quartz. J. Phys. C 4, 3265–3276.